Planar pixel sensors for the ATLAS upgrades at HL-LHC

Stefano Terzo
L. Andricek, A. Macchiolo, H.-G. Moser, R. Nisius,
R.-H. Richter and P. Weigell

MAX-PLANCK-GESELLSCHAFT

Max-Planck-Institut für Physik & Max-Planck-Institut Halbleiterlabor
München

Young Scientist Workshop
Ringberg Castle
23$^{\mathrm{th}}$ July 2013

The silicon pixel tracker

3 barrel layers
2×3 end cap disks

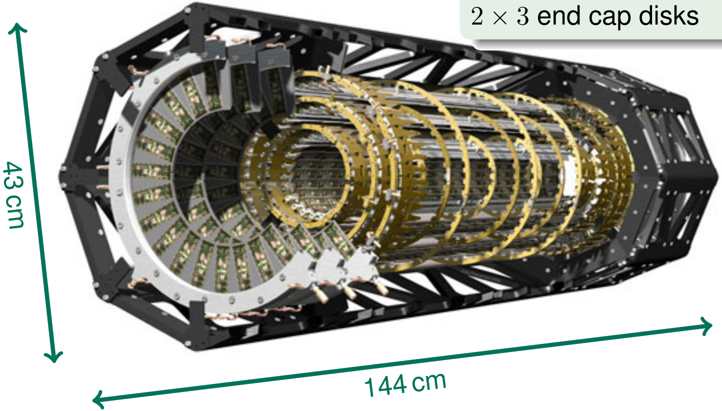

The pixel tracker challenge

$H \rightarrow b\bar{b}$

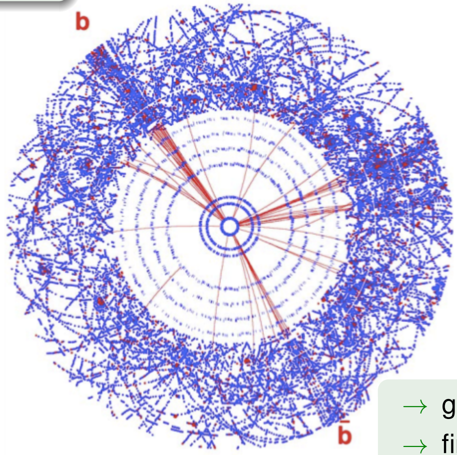

- $\rightarrow$ good momentum resolution
- $\rightarrow$ find secondary vertexes (b-tagging)

Hybrid silicon pixel detectors

- Pixel surface segmentation
  → True 2D spatial information
- Readout chip coupling (bump bonding)

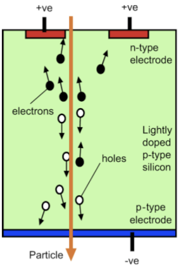

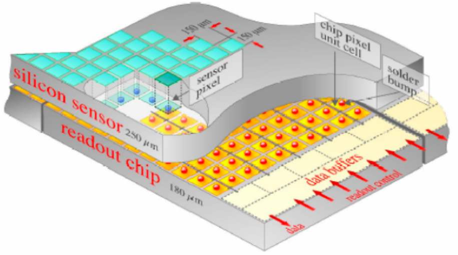

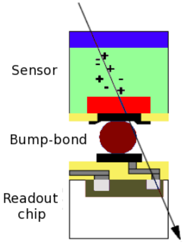

Hybrid silicon pixel detectors

- Pixel surface segmentation
  - → True 2D spatial information
- Readout chip coupling (bump bonding)

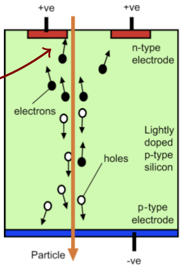

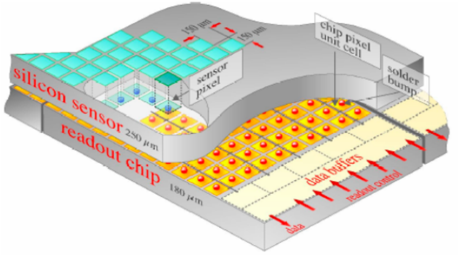

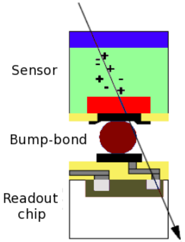

Hybrid silicon pixel detectors

- Pixel surface segmentation
  → True 2D spatial information
- Readout chip coupling (bump bonding)

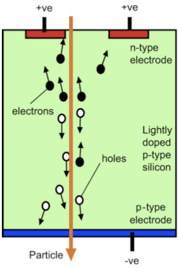

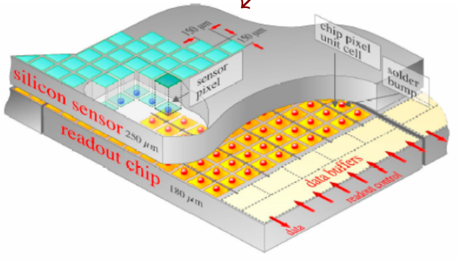

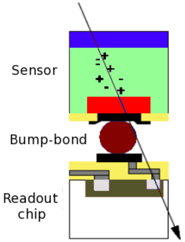

Hybrid silicon pixel detectors

- Pixel surface segmentation
  → True 2D spatial information

- Readout chip coupling (bump bonding)

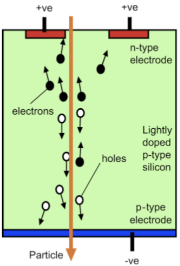

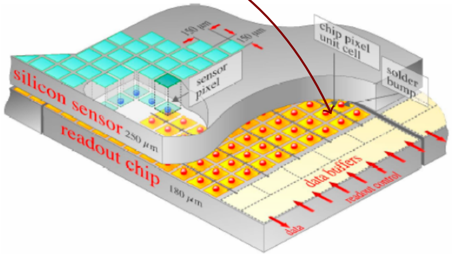

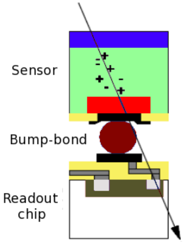

The present ATLAS pixels

- 1744 modules
- 46080 pixel channels per module: $50\,\mu\mathrm{m} \times 400\,\mu\mathrm{m}$
- n-in-n silicon sensors: 250μm thick
- FE-I3 readout chip
  - lowest threshold: ~ 3000 e$^-$
  - radiation hard up to $2{\times}10^{15}\mathrm{n_{eq}/cm^2}$

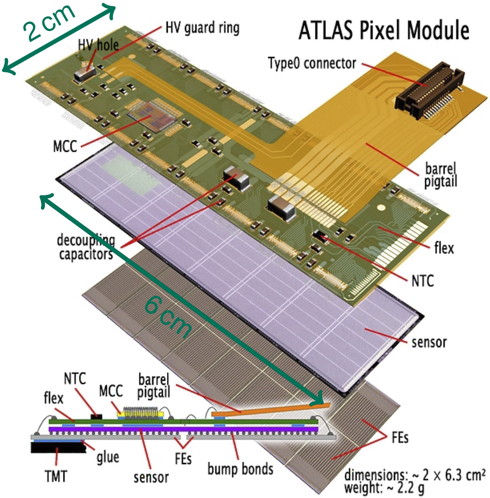

The inner tracker upgrade plan

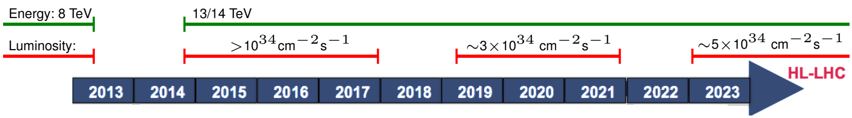

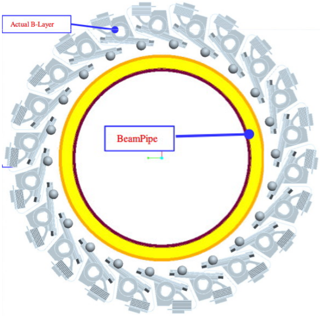

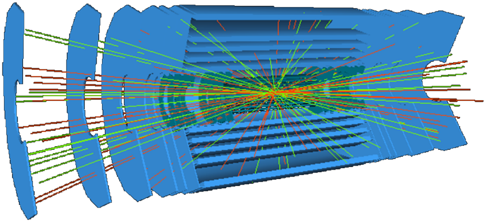

The inner tracker upgrade plan

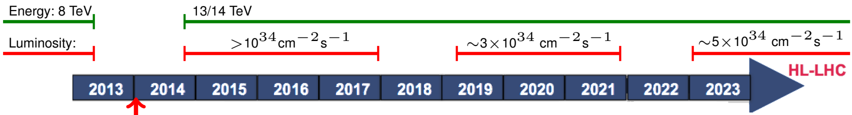

Insertable B-Layer (IBL): new pixel layer at 3.2 cm from the beam-pipe

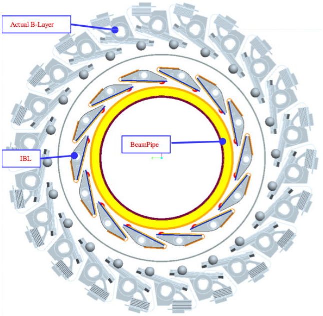

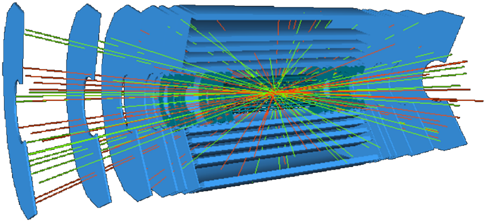

The inner tracker upgrade plan

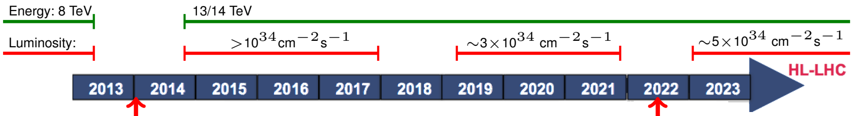

Insertable B-Layer (IBL): new pixel layer at 3.2 cm from the beam-pipe

"Phase II": full inner detector replacement (4-5 layers)

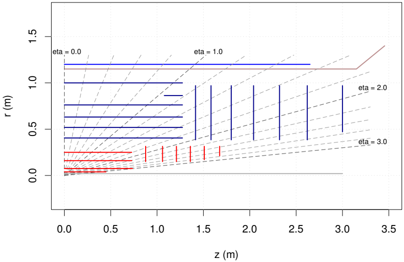

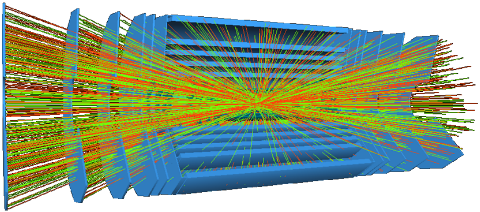

IBL and inner layers of Phase II

Advantages:

- better tracking precision, vertexing and b-tagging performance
- larger area covered along the beam line
- redundancy in the measurement of tracks

Problems:

- pileup $\rightarrow$ reduced occupancy

now: FE-I3 chip $400\times50\mu\mathrm{m}^2$

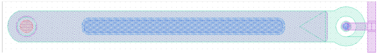

IBL: FE-I4 chip $250\times50\mu\mathrm{m}^2$

Ph. II: new chip $150\times25\mu\mathrm{m}^2$

- radiation damage

now: $\Phi_{eq} \sim 2\times10^{12}\mathrm{n_{eq}/cm^2}$
IBL: $\Phi_{eq} \sim 5\times10^{15}\mathrm{n_{eq}/cm^2}$
Ph. II: $\Phi_{eq} \sim 2\times10^{16}\mathrm{n_{eq}/cm^2}$

- dead area

$\rightarrow$ smaller overlapping space

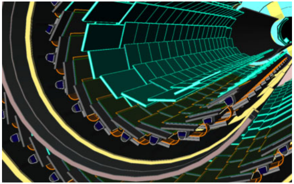

Our module concept for phase II

- the present ATLAS module design

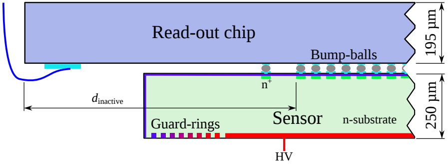

- active edges: maximize the active area of the sensor

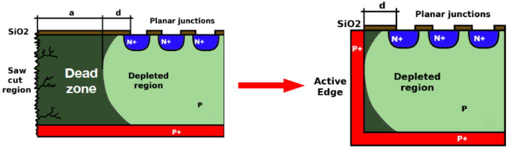

- InterChip Vias (ICV): bring the signal directly to the backside passing through the chip

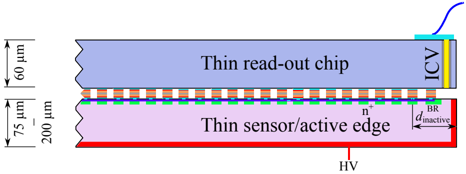

Planar active edge sensors

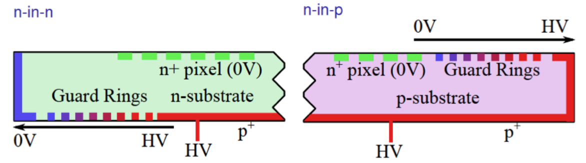

- present IBL design:
  - n-in-n sensor with 200 μm edge (pixel shifted under the guard rings)
- Phase II alternatives:
  - n-in-p sensor with 125 μm active edge (only one Bias Ring)
  - n-in-p sensor with 50 μm active edge (Floating Guard Ring)

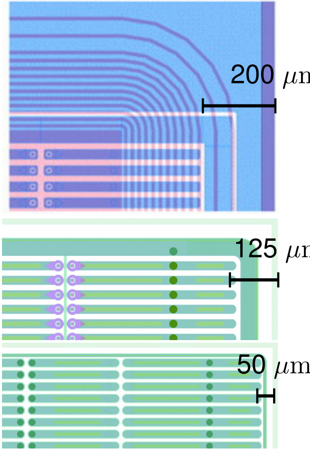

Hit efficiency for edge pixels

FE-I3 50 μm active edge

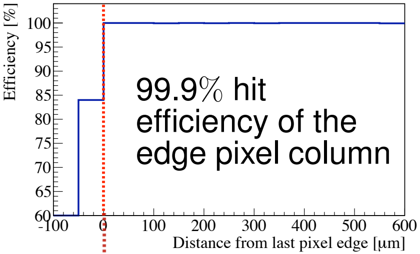

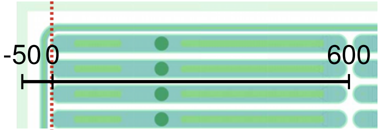

84$^{+9}_{-14}$% hit efficiency between the last pixel implant and the active edge

FE-I3 125 μm slim edge

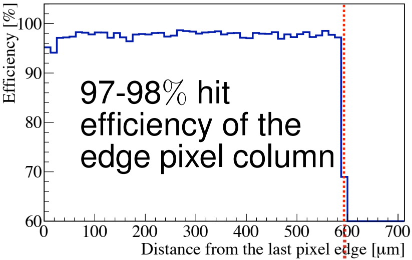

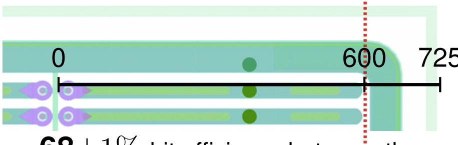

68$\pm$1% hit efficiency between the last pixel implant and the bias ring

Radiation damage in silicon detectors

Displacement of lattice atoms (crystal damage)

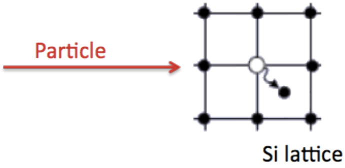

- **recombination centers**
  - $\rightarrow$ affect doping concentration

  } increase of depletion voltage
- **generation centers**
  - $\rightarrow$ increase of leakage current

  } noise increase
- **trapping centers**
  - $\rightarrow$ mean free path reduced
  - $\rightarrow$ decrease of charge collection efficiency

  } signal decrease

Our thin silicon detectors

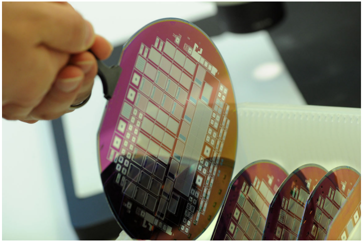

- from $200\,\mu m$ to $75\,\mu m$ thinned sensors
  - $\rightarrow$ lower trapping probability
  - $\rightarrow$ lower depletion voltage ($V_{\mathrm{dep}} \sim d^2$)
  - $\rightarrow$ less multiple scattering
- lower signals $\rightarrow$ new FE-I4 readout chip that allows lower thresholds

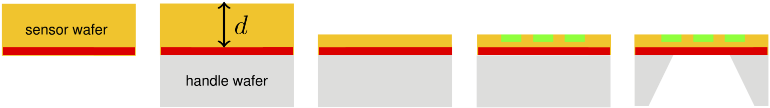

1. Implant backside on sensor
2. Bond sensor wafer to handle wafer
3. Thin sensor side to desired thickness
4. Process on top side
5. Structure resist, etch backside up to oxide/implant

Characterization setup in laboratory

- ^{90}Sr beta source
- external trigger via scintillator
- full setup cooled in a climate chamber from 20°C to -50°C

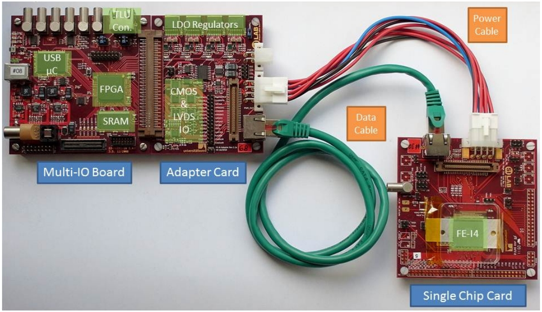

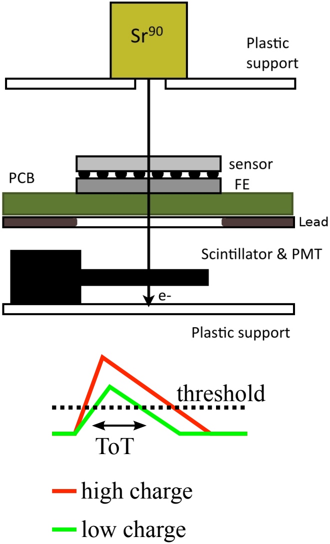

Charge Collection: thickness comparison

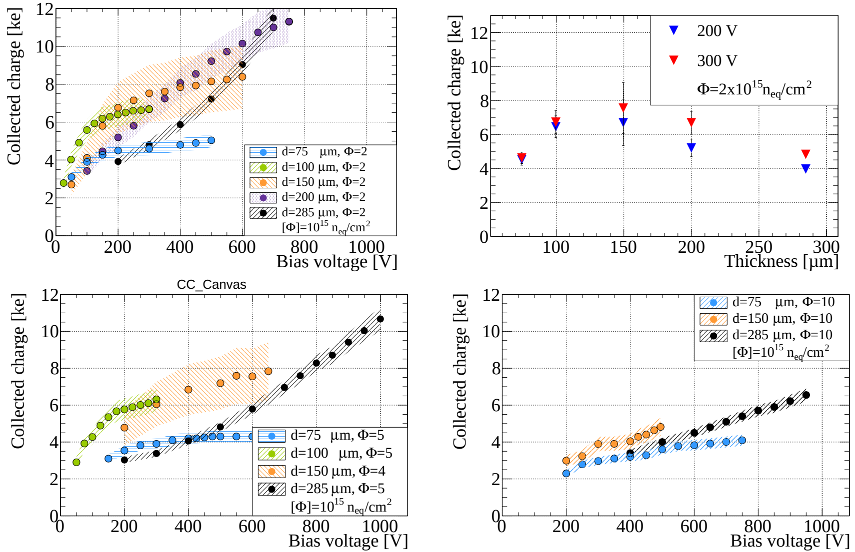

FE-I4 150 μm thick: hit efficiency

- Test-beam measurement:
  - at SpS, CERN with 120 GeV pions
  - at DESY, Hamburg with 4-6 GeV electrons

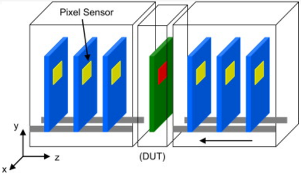

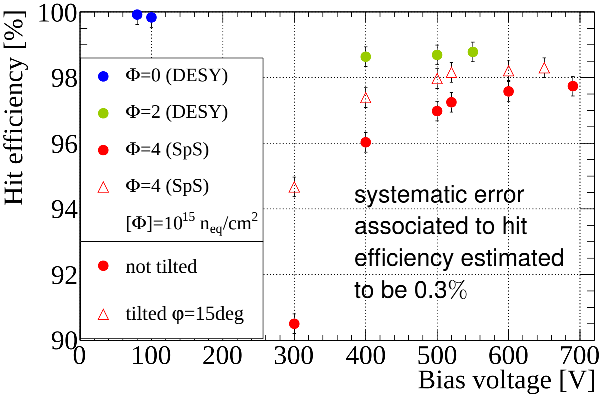

systematic error associated to hit efficiency estimated to be 0.3%

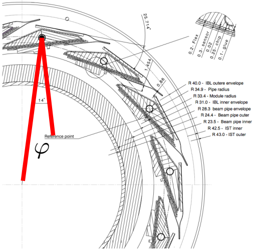

Hit efficiency at different η incidence

- **FE-I4 150 μm thick sensor, irradiated to 4$\times$10^{15}n_{eq}/cm^2**
- threshold: 1.6 ke

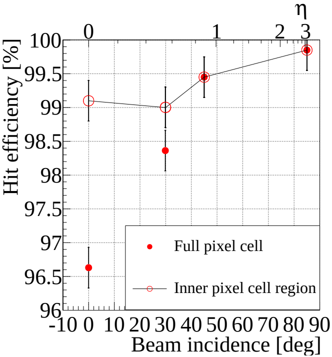

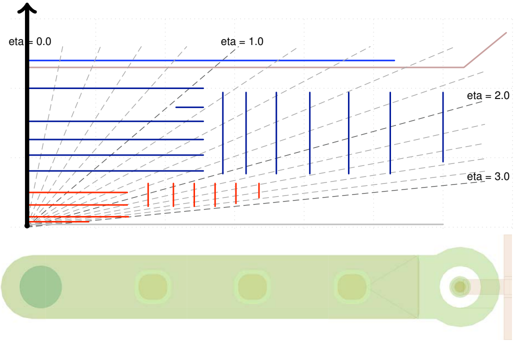

- 96.6% hit efficiency at $\perp$ incidence (500 V)

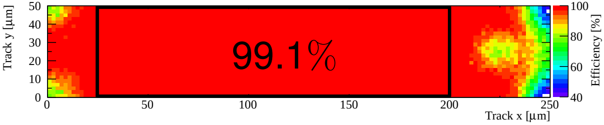

Hit efficiency at different η incidence

- **FE-I4 150 μm thick sensor, irradiated to 4$\times$10^{15}n$_{eq}$/cm^2**
- threshold: 1.6 ke

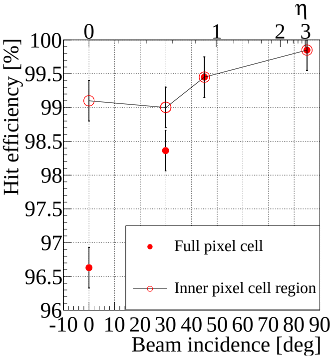

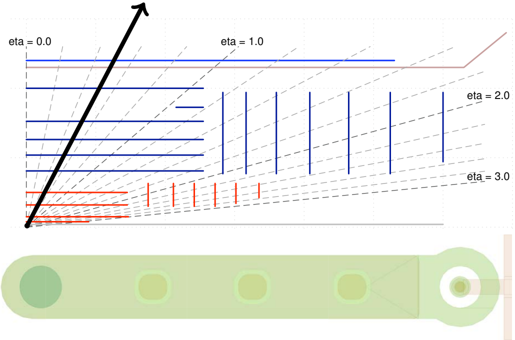

- 98.4% hit efficiency at ϑ=30° (η ~0.55) (500 V)

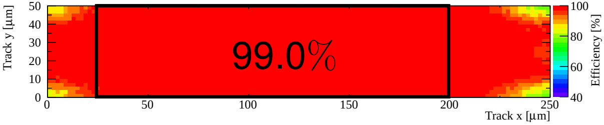

Hit efficiency at different η incidence

- **FE-I4 150 μm thick sensor, irradiated to 4$\times$10^{15} $\mathrm{n_{eq}/cm^2}$**
- threshold: 1.6 ke

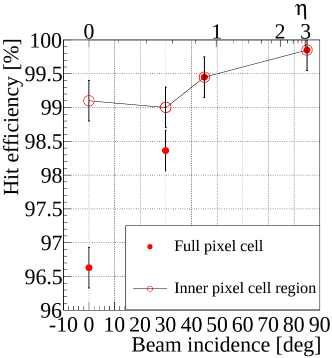

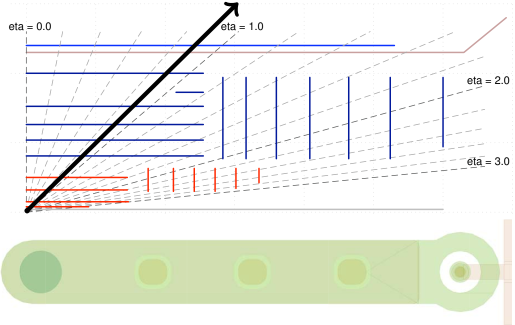

- 99.5% hit efficiency at ϑ=45° (η ~0.88) (500 V)

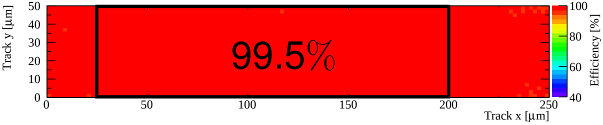

Hit efficiency at different η incidence

- **FE-I4 150 μm thick sensor, irradiated to 4$\times$10^{15}n$_{eq}$/cm^2**
- threshold: 1.6 ke

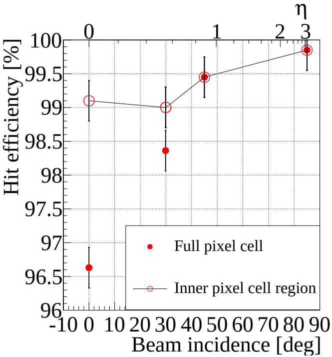

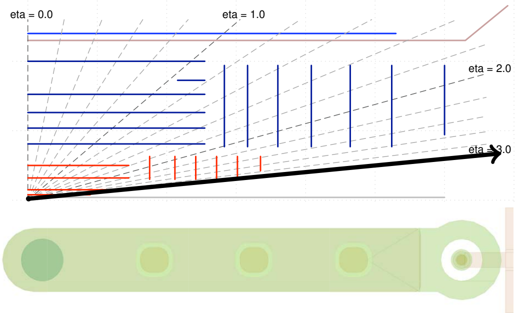

- 99.8% hit efficiency at ϑ=85° (η ~3.1) (500 V)

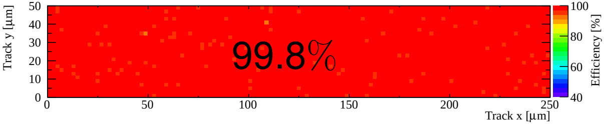

High-eta cluster properties

FE-I4 150 μm thick sensor, irradiated to 4$\times$10^{15}$\mathrm{n_{eq}/cm^2}$ (ϑ=85°)

- long clusters $\rightarrow$ higher occupancy
- threshold and under depletion effects

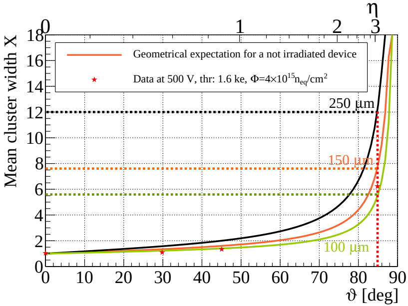

Mean cluster width expected along the tilted direction for different incidence angles

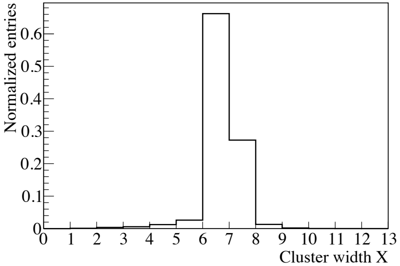

Cluster distribution along the tilted direction.

Distribution mean = 6.2

Conclusions and outlook

- Thin active edge sensors before irradiation have high efficiency even outside the pixel area
  - this allows the design of a fully active pixel detector without module overlap that can be placed closer to the beam-pipe
- Thin sensors (100 $\mu\mathrm{m}$ and 150 $\mu\mathrm{m}$) show very good performance up to $4\times10^{15}\mathrm{n_{eq}/cm^2}$ and are suited for the internal or intermediate layers of the Phase II upgrade

What's next:

- Further irradiations of the thin sensors up to $2\times10^{16}\mathrm{n_{eq}/cm^2}$ with neutrons and protons.
- More studies of the active edge sensors after irradiation.

Backup slides

What a silicon detector is

- A pure intrinsic semiconductor has equal electron and hole densities
  - Transferred energy:
    - $\rightarrow$ electron exited from the valence to the conduction band
    - $\rightarrow$ MIP: $\sim 8000\,\mathrm{e}^{-}$-h pairs $\times 100\,\mu\mathrm{m}$

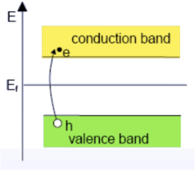

- Doping $\rightarrow$ introduce impurities in the Si lattice:

n-type:

- $\rightarrow$ free electrons
- $\rightarrow$ Fermi level near the Conduction Band

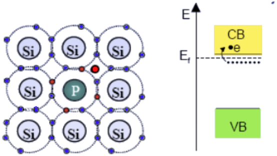

p-type:

- $\rightarrow$ free holes (electron vacancies)
- $\rightarrow$ Fermi level near the Valence Band

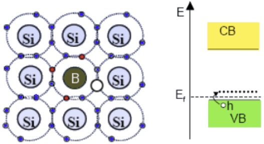

What a silicon detector is

- A pure intrinsic semiconductor has equal electron and hole densities
  - Transferred energy:
    - $\rightarrow$ electron exited from the valence to the conduction band
    - $\rightarrow$ MIP: $\sim 8000\,$e^{-}-h pairs $\times 100\,\mu\mathrm{m}$

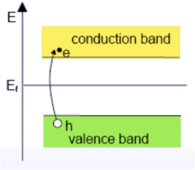

- Doping $\rightarrow$ introduce impurities in the Si lattice:

n-type:

- $\rightarrow$ free electrons
- $\rightarrow$ Fermi level near the Conduction Band

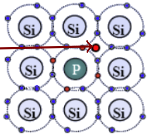

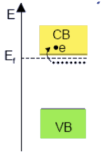

p-type:

- $\rightarrow$ free holes (electron vacancies)
- $\rightarrow$ Fermi level near the Valence Band

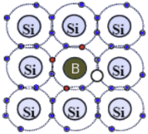

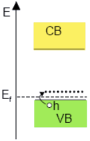

What a silicon detector is

- A pure intrinsic semiconductor has equal electron and hole densities
  - Transferred energy:
    - → electron exited from the valence to the conduction band
    - → MIP: $\sim 8000\,\mathrm{e}^{-}$-h pairs $\times 100\,\mu\mathrm{m}$

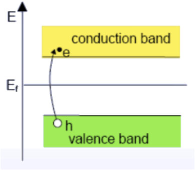

- Doping → introduce impurities in the Si lattice:

n-type:

→ free electrons

→ Fermi level near the Conduction Band

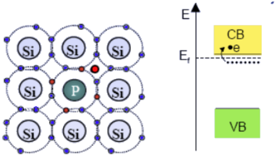

p-type:

→ free holes (electron vacancies)

→ Fermi level near the Valence Band

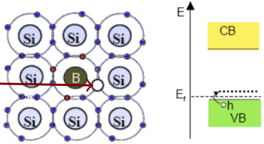

Reversed bias p-n junction

- p-n junction:
  - → there must be a single Fermi level
  - → band structure deformation
  - → potential difference in the junction
  - → charge flows until the equilibrium

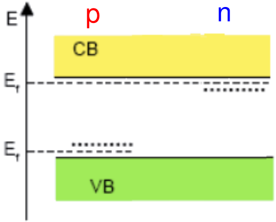

- Reversed bias:
  - → increase of the depletion zone
  - → depleted zone = sensitive volume
  - → $V_B > V_{\text{dep}} \rightarrow$ maximum collected charge

Reversed bias p-n junction

- p-n junction:
  - → there must be a single Fermi level
  - → band structure deformation
  - → potential difference in the junction
  - → charge flows until the equilibrium
- Reversed bias:
  - → increase of the depletion zone
  - → depleted zone = sensitive volume
  - → $V_B > V_{\mathrm{dep}} \rightarrow$ maximum collected charge

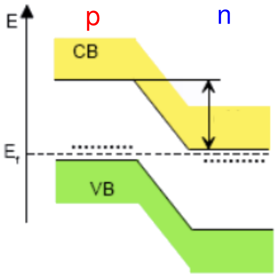

Reversed bias p-n junction

- p-n junction:
  - → there must be a single Fermi level
  - → band structure deformation
  - → potential difference in the junction
  - → charge flows until the equilibrium
- Reversed bias:
  - → increase of the depletion zone
  - → depleted zone = sensitive volume
  - → $V_B > V_{\mathrm{dep}} \rightarrow$ maximum collected charge

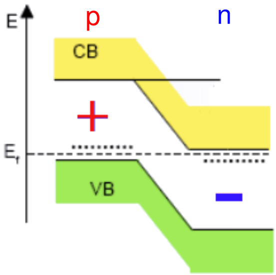

Reversed bias p-n junction

- p-n junction:
  - $\rightarrow$ there must be a single Fermi level
  - $\rightarrow$ band structure deformation
  - $\rightarrow$ potential difference in the junction
  - $\rightarrow$ charge flows until the equilibrium
- Reversed bias:
  - $\rightarrow$ increase of the depletion zone
  - $\rightarrow$ depleted zone = sensitive volume
  - $\rightarrow$ $V_B > V_{\mathrm{dep}}$ $\rightarrow$ maximum collected charge

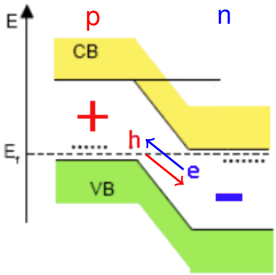

Reversed bias p-n junction

- p-n junction:
  - $\rightarrow$ there must be a single Fermi level
  - $\rightarrow$ band structure deformation
  - $\rightarrow$ potential difference in the junction
  - $\rightarrow$ charge flows until the equilibrium
- Reversed bias:
  - $\rightarrow$ increase of the depletion zone
  - $\rightarrow$ depleted zone = sensitive volume
  - $\rightarrow$ $V_B > V_{\mathrm{dep}} \rightarrow$ maximum collected charge

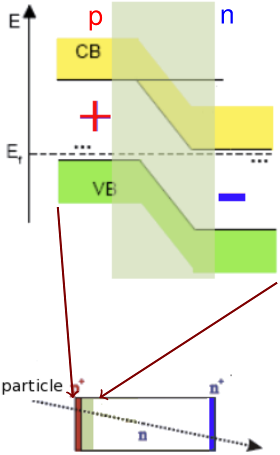

Reversed bias p-n junction

- p-n junction:
  - → there must be a single Fermi level
  - → band structure deformation
  - → potential difference in the junction
  - → charge flows until the equilibrium

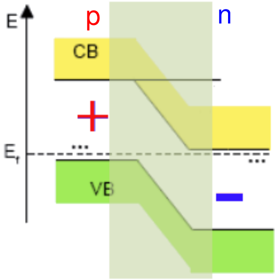

- Reversed bias:
  - → increase of the depletion zone
  - → depleted zone = sensitive volume
  - → $V_B > V_{\text{dep}}$ → maximum collected charge

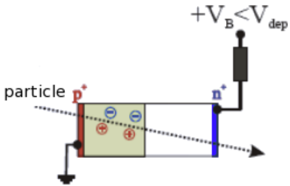

Reversed bias p-n junction

- p-n junction:
  - → there must be a single Fermi level
  - → band structure deformation
  - → potential difference in the junction
  - → charge flows until the equilibrium
- Reversed bias:
  - → increase of the depletion zone
  - → depleted zone = sensitive volume
  - → $V_B > V_{\mathrm{dep}}$ → maximum collected charge